ELSEVIER

Journal of Structural Geology 29 (2007) 1632–1649

JOURNAL OF STRUCTURAL GEOLOGY

www.elsevier.com/locate/jsg

# Two orogens – One shear belt: 1 Ga of repeated deformation along the Central Tanzanian Shear Belt

Veronika Tenczer*, Harald Fritz, Andreas Bauernhofer, Christoph Hauzenberger

*Institute for Earth Sciences, University of Graz, Universitätsplatz 2, 8010 Graz, Austria*

Received 25 January 2007; received in revised form 18 June 2007; accepted 18 June 2007
Available online 6 July 2007

**Abstract**

The Central Tanzanian Shear Belt (CTSB) constitutes a 300-km long W–E trending dextral shear belt that was active during Paleoproterozoic and Neoproterozoic orogenies. It formed along the southern margin of the Archean Tanzania Craton that acted as rigid indenter during both orogenies. Based on structural and microtextural methods several deformational stages have been identified. Paleoproterozoic shear is recorded in the 1.8–2.0 Ga old magmatic Usagaran Belt. This shear was accompanied by vast melt intrusions in a hot and soft crust leading to low strain and coaxial flow. It ceased in an exhumation phase with localized non-coaxial shear followed by the deposition of nonconform sediments dated around 1.9 Ga. In the Neoproterozoic, the CTSB is found as reactivated shear zones in the Usagaran Orogen and as megascale shear zone in the metamorphic Mozambique Belt. It is a release (or counterflow) structure that evolved in the course of crustal thickening in a strong crust around 0.6 Ga. Along the strike of the Neoproterozoic CTSB syntectonic conditions change from localized brittle shear along the Tanzania Craton to distributed high temperature coaxial shear in the eastern section of the orogen's root. This goes along with a significant change in microstructures and LPO patterns.



*Keywords:* Central Tanzanian Shear Belt; Paleoproterozoic, Neoproterozoic deformation; Usagaran; Mozambique Belt; Lattice preferred orientation

## 1. Introduction

Mobile belts and crustal-scale shear zones frequently evolve along or parallel to pre-existing structures and can be found worldwide throughout the geological history. In the Precambrian mobile belts of Tanzania some of these megascale shear zones penetrate different crustal levels and offer the possibility to reconstruct their complex tectonic history and their role during Proterozoic plate tectonics. Despite the fact that the East African mobile belts have been intensely studied in the past mainly by geochronological, geochemical and petrological means (Wendt et al., 1972; Kröner, 1977; Maboko, 2000; Möller et al., 2000; Muhongo et al., 2001; Reddy et al., 2003, 2004; Collins et al., 2004; Collins and Pisarevsky, 2005; Tenczer et al., 2006) there is only little knowledge about the existence and the structural evolution of their associated shear belts (Hepworth, 1972; Daly, 1988; Shackleton, 1973; Fritz et al., 2005).

Recent studies revealed the existence of several W–E trending crustal-scale shear belts that cut the overall N–S trend of the East African Orogen and that were possibly repeatedly active in the Proterozoic (Fritz et al., 2005). Shear fabrics extend over some 100 km from the margin of the Tanzania Craton in the west and continue eastwards through the Paleoproterozoic Usagaran and the Neoproterozoic Mozambique Belt. One of these shear belts has been defined as Central Tanzanian Shear Belt (CTSB) by Fritz et al. (2005) (Fig. 1). The CTSB was identified as release structure during the collision of East- and West-Gondwana governed by the indentation of the Tanzanian Craton in the Neoproterozoic. It has been shown that along the CTSB relic Paleoproterozoic shear fabrics are found in the Usagaran Belt.

In this study, we provide a detailed structural and microtextural analyses of the CTSB with focus on the Paleoproterozoic Usagaran Belt and its Neoproterozoic overprint along the

* Corresponding author.
*E-mail address:* tenczer@uni-graz.at (V. Tenczer).

0191-8141/$ - see front matter © 2007 Elsevier Ltd. All rights reserved.
doi:10.1016/j.jsg.2007.06.004

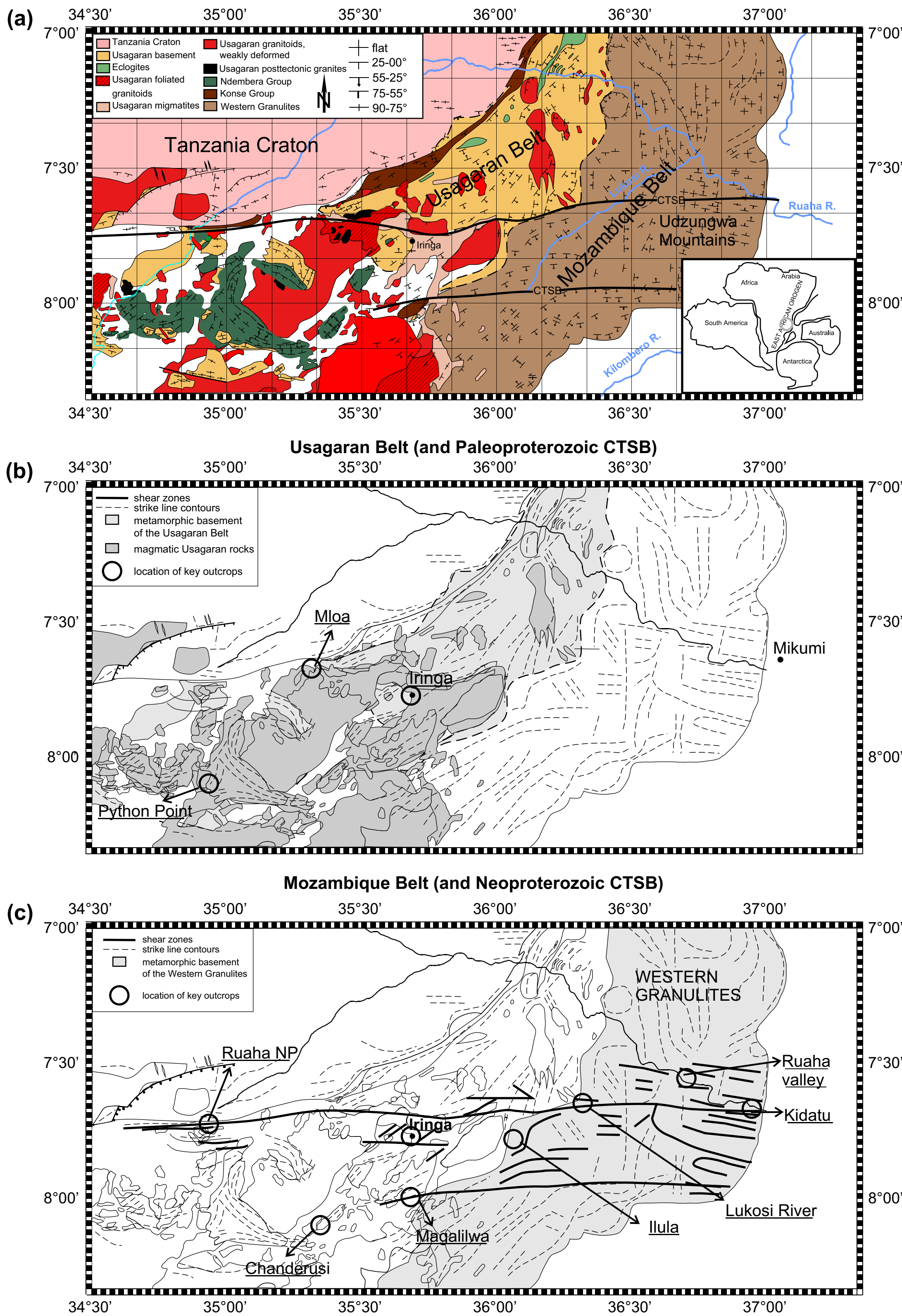


Fig. 1. (a) Lithological units as well as strike and dip in the study area compiled from the available geological maps from the Geological Survey of Tanzania. Insert shows the position of the study area in a sketch outlining Gondwana. The Usagaran granitoids are redrawn after Wendt et al. (1972). (b) The location of key outcrops in the Usagaran Belt is given on a map showing the strike line contours and shear zones that can be inferred as Paleoproterozoic relics of the CTSB. (c) Location of key outcrops and strike line contours in the Neoproterozoic CTSB. The Neoproterozoic CTSB is outlined. The coordinates of the outcrops are the following: Ruaha NP: S 7°42′59.1″ E 34°54′00.0″; Mloa: S 7°39′26.7″ E 35°24′12.1″; Iringa: S 7°42′27.9″ E 35°43′54.9″; Python Point: S 8°08′50.4″ E 35°01′37.5″; Chanderusi: S 8°02′52.8″ E 35°25′47.0″; Magalilwa: S 8°00′31.3″ E 35°42′16.3″; Ilula: S 7°40′12.7″ E 36°03′03.9″; Lukozi River: S 7°35.466′ E 36°20.125′; Ruaha River valley: S 7°34′32.2″ E 36°45′13.5″; Kidatu: S 7°38′34.6″ E 36°53′56.6″.

southern margin of the Tanzania Craton. This area is largely unexplored but allows excellent insight into the complex history of Paleoproterozoic tectonics in East Africa. We discuss the mechanisms behind the localization and reactivation of large-scale shear zones that form particular geometries in the different crustal levels at different times. Furthermore, we compare our results with the kinematic model from the study area suggested by Daly (1988). Our methodical approach is a structural study based on detailed field work at outcrop scale. Several key outcrops are discussed where the different stages of tectonic evolution of the CTSB can be inferred. Kinematics, deformation mechanisms and rheology are deduced from thin sections with analyses of microstructures and lattice preferred orientation patterns of rock forming minerals.

## 2. Geological framework

The study area is part of the East African Orogen (Stern, 1994), which is a north–south striking belt, that formed during the Neoproterozoic collision of West- and East-Gondwana fragments. This mobile belt can be traced along several thousands of kilometres along East Africa exposing largely upper crustal sequences in the northern part (Arabian Nubian Shield) and lower crustal sequences in the south (Vail, 1985; Stern, 1994). In Tanzania the East African Orogen is also referred to as Mozambique Belt, which formed by westward nappe stacking onto the Archean Tanzania Craton during the Neoproterozoic at ca. 640 Ma (Möller et al., 2000; Muhongo et al., 2001; Sommer et al., 2003; Fritz et al., 2005). Along the southeastern margin of the Tanzania Craton the Neoproterozoic nappe sequence is not in direct contact with the Archean Craton. Here, the Mozambique Belt is tectonically juxtaposed to the pre-existing Paleoproterozoic Usagaran Belt along a stepwise boundary (Fig. 1a). The Usagaran orogeny occurred around 1.8–2.0 Ga, approximately coeval with the consolidation of other Paleoproterozoic terranes, e.g. the Ubendian Belt, exposed to the southwest of the Tanzanian Craton (Daly, 1988). The Usagaran Orogen is a predominately magmatic belt (Wendt et al., 1972; Maboko and Nakamura, 1996; Collins et al., 2004) with its widest extension south to southeast of the Tanzania Craton. There are some major differences between the broad southern Usagaran Belt (where the CTSB is localized) and the narrow Northern Usagaran Belt (along the N–S trending Craton boundary). The Southern Usagaran Belt is dominated by magmatic rocks, e.g. granodiorites, monzogranodiorites and tonalities that intruded a metamorphic basement mainly consisting of felsic orthogneisses and migmatites. Wendt et al. (1972) have intensely studied these magmatites and classified the "Usagaran granitoids" into three different types: pre-, syn- or post-Usagaran magmatic bodies. According to Wendt et al. (1972) the granitoids can be divided into a (1) foliated type, (2) weakly deformed type and (3) undeformed post-tectonic granitoids (Fig. 1a). A cover sequence within the southern Usagaran Belt is the volcano–sedimentary Ndembera Group, constrained at ca. 1.9 Ga (Wendt et al., 1972; Collins et al., 2004; Sommer et al., 2005b). We consider the Ndembera Group as an important time marker because it nonconformly overlies the Usagaran metamorphic basement and partly the granitoids. The succession consists of acidic (andesitic) tuffs, dacites and rhyolites and low-grade metamorphosed sediments (quartzites and shales). Sedimentary cover sequences are also found as thin, sheared slices along the boundary of the Craton (Konse Group) and along the Usagaran/Mozambique Belt boundary south of Iringa (Magalilwa Group) (Fig. 1). Both sedimentary groups mainly consist of muscovite-bearing quartzites and conglomerates. The Konse Group has been stratigraphically correlated with the Ndembera Group (Mruma, 1995).

Northwards, along the eastern margin of the Tanzania Craton the Usagaran Belt becomes much narrower and changes its strike from NE–SW to N–S orientation (Fig. 1a). Here the rock suite is dominated by pre-intrusive metamorphic basement composed of migmatic gneisses, metasedimentary sequences but also 2.0 Ga old eclogites. Eclogite facies was overprinted by amphibolite facies metamorphism at >1991 Ma (Collins et al., 2004; Möller et al., 1995). The northern Usagaran Belt is also strongly influenced by greenschist facies deformation during westward Neoproterozoic nappe emplacement onto the Tanzania Craton and has therefore a different structural style (Reddy et al., 2003).

To the east of the Usagaran Belt, the Western Granulites of the Mozambique Belt are exposed (Fig. 1c). These are metamagmatic and metasedimentary rocks (metapsammites and metapelites), mainly reworked from the Tanzania Craton and the Usagaran Belt and metamorphosed during the Neoproterozoic orogenic cycle (e.g. Sommer et al., 2005a; Vogt et al., 2006). The structural style of the Mozambique Belt is characterized by forward propagation of thrusts emplaced onto the Tanzania Craton with deepening of the basal decollement level from west to east (Reddy et al., 2003; Fritz et al., 2005). The westernmost section of the Western Granulites exhibits gneisses with greenschist to lower amphibolite facies whereas in the east granulites facies rocks are found. The Neoproterozoic tectonics resolved in different structures north and south of the Ruaha River valley in the Western Granulites (Fig. 1c). North of the Ruaha River a flat-lying thrust and fold belt developed with north–south oriented strike line contours. South of the Ruaha River valley strike line contours show an arcuate bending that grades from N–S to W–E strike approaching the Ruaha River valley. This deflection of strike lines has previously been interpreted as response to shear along the CTSB (Fritz et al., 2005).

The boundary between the Usagaran and the Mozambique belts is mainly defined by the first regional appearance of Neoproterozoic mica cooling ages (Wendt et al., 1972) and penetrative ductile Neoproterozoic deformation (Fritz et al., 2005). The easternmost units of the Mozambique Belt in Tanzania comprise the Eastern Granulites, which are defined as a different Meso/Neoproterozoic terrane (Fritz et al., 2005). These units are not discussed here.

## 3. Methodology

The structural study scales down from map scale over outcrop observations to the analyses of microstructures and

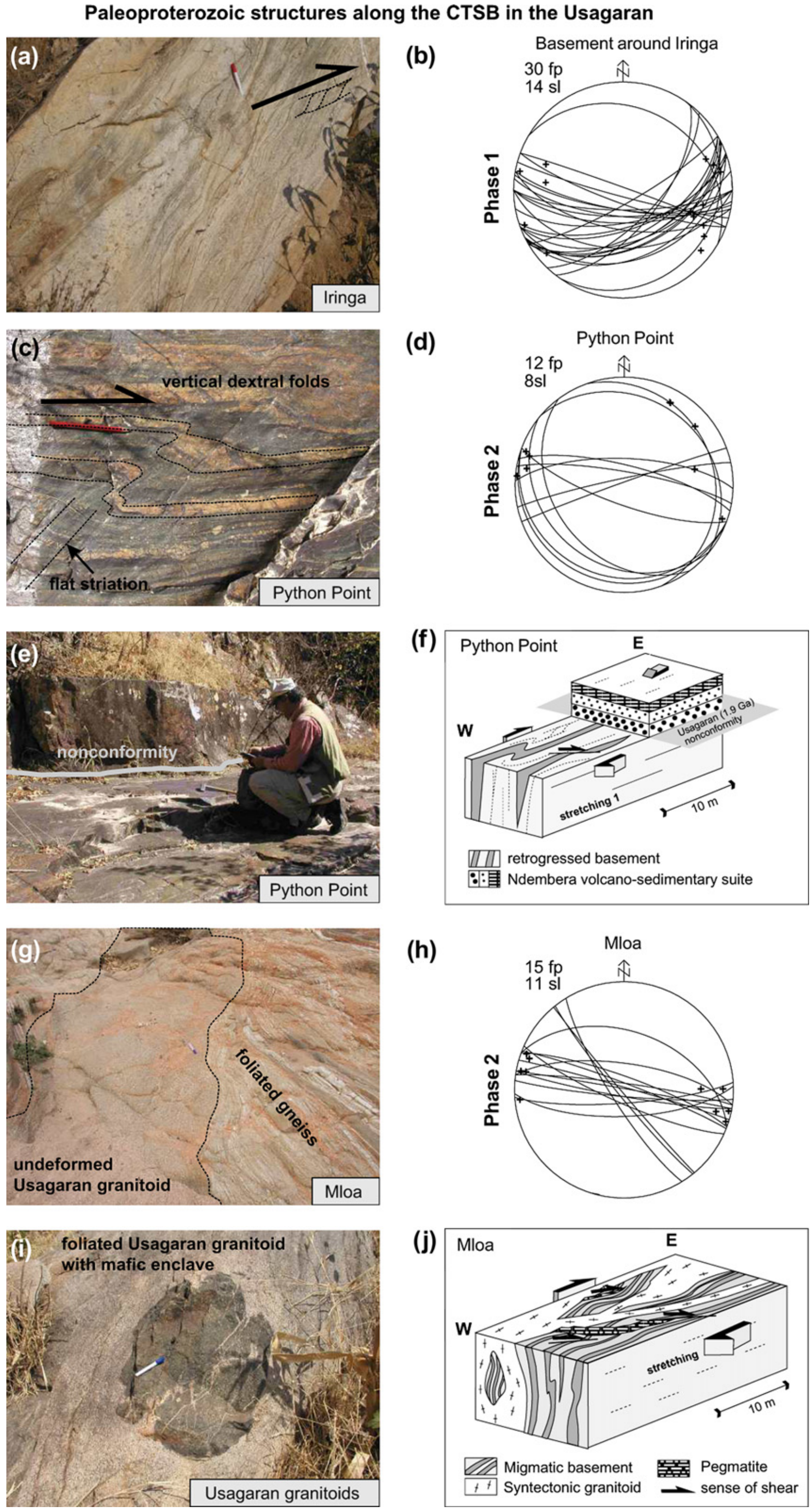


Fig. 2. Representative outcrop photographs and structural data from locations, where the Paleoproterozoic tectonics is seen along the CTSB in the Usagaran Belt. Structural data are shown in lower hemisphere equal area plots of foliation planes (fp) and stretching lineation (sl). Foliation (great circles) and lineation (cross) forms are given for key outcrops. (a) Migmatic basement gneisses around Iringa with melt schlieren and s−c fabrics in the non-migmatic part of the rock indicating dextral shear. (b) Structural data for the Usagaran Basement around Iringa. (c) The steeply dipping banded orthogneisses close to Python Point show dextral shear of ductile folds in dm-scale. The dark bands are mainly composed of retrograde minerals like epidote and chlorite. This fabric occurs immediately below the nonconformity to flat-lying quartzitic sediments that have been deposited coeval with the Ndembera succession. (d) Structural data for the key area Python Point containing both, steeply dipping strike slip zones and data of the flat-lying nonconformity. (e) The co-author Harald Fritz working on the nonconformity at the outcrop Python Point. (f) Summarizing sketch with the main structural features of the outcrop Python Point. (g) This outcrop close to Mloa is an excellent example for the timing of deformation. The foliated gneiss has been deformed before the Usagaran granitoid intruded around 1.8 Ga (Wendt et al., 1972). No later overprint can be seen. (h) Summarizing sketch with the main structural features of the outcrop Mloa.

mineral textures. Map scale observations cover a stripe of ca. $200 \times 50$ km and aim to identify widths, trend and geometry of the CTSB. The study on outcrop structures includes classical overprint criteria to distinguish succession of structural events. An important role to elaborate Paleoproterozoic and Neoproterozoic tectonic features takes the ca. 1.9 Ga old Ndembera Group. This single deformed volcano–sedimentary suite nonconformly overlies an intensely deformed basement. In addition time relations between pluton emplacement and tectonics have been used to put relative age constraints on deformation. From ca. 200 studied outcrops along the CTSB key outcrops were selected that show typical structural association of Paleoproterozoic and Neoproterozoic events.

The microstructural analysis was performed to constrain and approve sense of shear and succession of events, but even more important, to put constraints on the variation of temperature dependent deformation mechanisms. We follow the systematic given by Stipp et al. (2002) that has been adopted by Fritz et al. (2005) for the requirement of the study area. In general, we distinguish with rising temperature conditions a change from bulging (BG), subgrain rotation (SR), grain boundary migration (GBM) and diffusional processes.

Selected samples were studied for lattice preferred orientation (LPO) pattern of quartz by the use of a conventional U-stage and X-ray texture goniometry. Polished rock chips were placed in the X-ray beam of a Bruker AXS texture goniometer (wavelength $\mathrm{CuK}\alpha = 1.5418$, beam current = 40 kV and 40 mA) used in reflection mode. Eight lattice planes ($\langle 100\rangle$, $\langle 110\rangle$, $\langle 102\rangle$, $\langle 200\rangle$, $\langle 201\rangle$, $\langle 112\rangle$, $\langle 211\rangle$, $\langle 113\rangle$) have been directly measured, lattice planes $\langle 001\rangle$, $\langle 101\rangle$ and $\langle 011\rangle$ were calculated using the orientation density function (ODF) based on the harmonic method of Roe (1965) and Bunge (1981). Quartz $c$-axes and $\langle a\rangle$-axes from which crystal glide plane and glide direction are commonly inferred are displayed on stereo plots. For detailed description of the technical procedure see Wenk (1985).

LPO patterns, although influenced by strain rate, grain size, fluid activity, etc., provide information on temperature dependent glide systems and kinematics (e.g. Lister and Hobbs, 1980; Schmid and Casey, 1986; Kruhl, 1996; Passchier and Trouw, 1996; Law et al., 2004), the flow geometry and the quality (i.e. vorticity) of flow (e.g., Vissers, 1989; Law et al., 1990; Wallis, 1992) and thus complete the microstructural study. The flow geometry is inferred from quartz $c$-axes patterns in which the central girdle segment develops orthogonal to the flow plane in both simple and general shear (Lister and Hobbs, 1980; Platt and Behrmann, 1986; Vissers, 1989; Law et al., 1990; Wallis, 1992). Under these assumptions the angle ($\beta$) between the perpendicular girdle to the central girdle and the foliation is equal to the angle between the flow plane and the flattening plane of strain and may be used to estimate the mean kinematic vorticity of flow (Wallis, 1992; Grasemann et al., 1999). Information on the strain geometry can be obtained from $\langle a\rangle$-axes patterns. Accepting models that predict $\langle a\rangle$-axes to represent direction of flow, maxima distributed along the periphery of the stereo plot are interpreted to represent deformation close to plane strain (Lister and Williams, 1979). Consequently, non-peripheral $\langle a\rangle$-axes maxima are considered as hint for three-dimensional, nonplane strain deformation.

## 4. Paleoproterozoic tectonics along the CTSB

A striking feature of the Southern Usagaran is that the majority of the exposed rock volume is made up of magmatics mainly derived from calcalkaline rocks. These include the metamorphic basement (migmatites and orthogneisses) that is deformed at high temperature conditions. Variably deformed granitoids intruded this basement around 1.8 Ga and occasionally the cover which is represented by the 1.9 Ga old volcano–sedimentary Ndembera Group. These magmatic rocks are important time markers in order to identify relics of Paleoproterozoic structures along the CTSB.

### *4.1. Field observations and macrostructures*

#### *4.1.1. Basement (around Iringa)*

Deformation in the Usagaran Basement generally produced high temperature (HT) fabrics including vertical, W–E to NE–SW trending foliation planes as seen in the area around Iringa (Fig. 2a, b). A HT dextral shear belt is defined from shear fabrics. The majority of basement rocks constitutes felsic gneisses composed of quartz, plagioclase, K-feldspar and biotite that occasionally display migmatic segregation. Mafic xenoliths (pyroxenite and amphibolite) are also incorporated into shear tectonics. In the migmatite deformation intensity was low and partly assisted by melt (low strain melt enhanced

Fig. 3. Photomicrographs from thin sections with typical microstructures and mineral assemblages of the key areas for Paleoproterozoic CTSB features in the Usagaran Belt. The images generally show sections parallel to the stretching lineation and perpendicular to the foliation. Mineral abbreviations are: Kfs, K-feldspar; Pl, plagioclase; Fsp, feldspar; Qtz, quartz; Ms, muscovite; SR, subgrain rotation; GBM, grain boundary migration; and D, disc quartz. (a) The migmatic gneisses of the Usagaran Basement exhibit high temperature deformation as shown by core-mantle structures of Kfs and grain boundary migration of Qtz. (b) Ribbon quartz is a typical feature for the Usagaran Basement gneisses. (c–f) Lower hemisphere equal area plots showing the preferred orientation of quartz ($\langle c\rangle$- and corresponding $\langle a\rangle$-axes) for the Paleoproterozoic (Pre-Ndembera) deformational phases found along the CTSB. Thin sections of the quartz fabric of the various samples are added. (c, d) MB262: Usagaran Basement from Dabaga. (e, f) MB288: Python Point. In thin section this is a previous mylonitic augengneiss from the Usagaran Basement (below the nonconformity at Python Point), which is intensely retrogressed by greenschist minerals like Chl, Ep and saussurite in Pl. In all diagrams the trace of foliation that approximates the maximum extension direction $X$ is oriented W–E, $Y$ is the centre and $Z$, the direction of minimum extension is N–S. Contoured lines are multiples of random. (g) This quartzitic sandstone is deposited on the nonconformity at Python Point. (h) An example for the Ndembera volcanics. Lithic fragments and an idiomorphic Pl-column flow in a fine-grained to glassy matrix of this ignimbritic rock type. The original rock fabric is only mildly deformed and metamorphosed as seen in very fine-grained Ms growth in the strain caps around Pl.

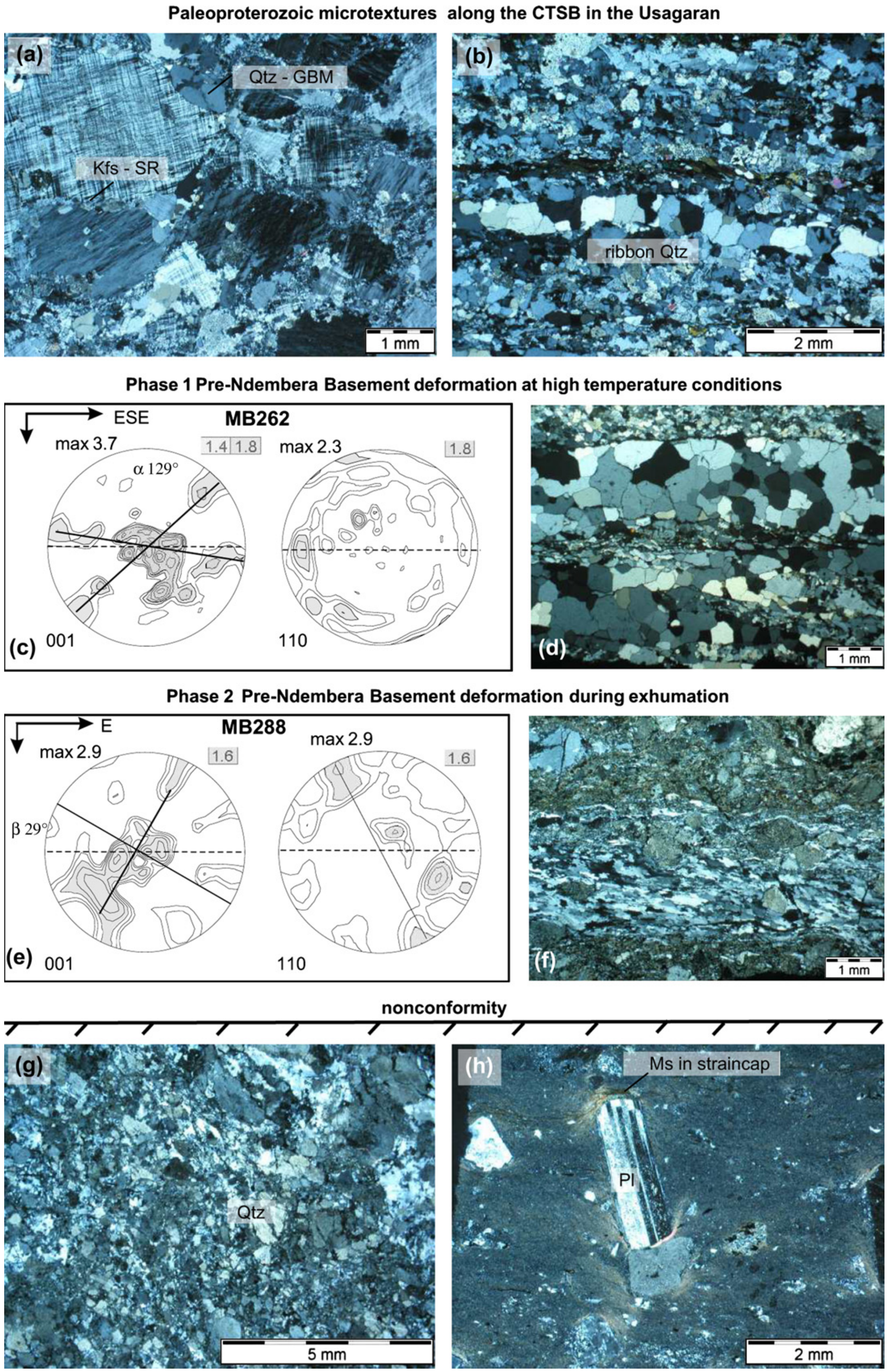
Paleoproterozoic microtextures along the CTSB in the Usagaran
(a)
Qtz - GBM
Kfs - SR
1 mm
(b)
ribbon Qtz
2 mm
Phase 1 Pre-Ndembera Basement deformation at high temperature conditions
ESE
MB262
max 3.7
1.4 1.8
max 2.3
1.8
α 129°
(c) 001
110
(d)
1 mm
Phase 2 Pre-Ndembera Basement deformation during exhumation
E
MB288
max 2.9
1.6
max 2.9
1.6
β 29°
(e) 001
110
(f)
1 mm
nonconformity
(g)
Qtz
5 mm
(h)
Ms in straincap
Pl
2 mm

deformation) characterized by schlieren and melt segregation. This initial deformation phase is referred to as phase 1.

*4.1.2. Basement–cover relationship (Python Point)*

A nonconformity between Usagaran Basement and cover is well exposed in a spectacular outcrop called Python Point (Figs. 1b, 2c–f). Here the basement gneisses display a vertical, W–E trending mylonitic foliation with a depositional contact to weakly metamorphosed, horizontally bedded sandstones and tuffs (Ndembera Group). The W–E trending mylonitic shear zone is composed of basement gneisses (augengneisses and amphibolites) below the depositional contact. Dextral sense of shear is inferred from strain shadows around feldspar, s–c fabrics and intrafolial shear folds (Fig. 2c). The mylonitic foliation is associated with a pronounced horizontal stretching lineation and significant strain (Fig. 2d). This deformation occurred at lower temperature conditions compared to phase 1 and is referred as phase 2. An initially amphibolite facies fabric was intensely retrogressed during deformation phase 2 as indicated by the growth of chlorite and epidote either parallel to the foliation or in cross-cutting tension gashes. This retrogression can be correlated with exhumation prior to the onset of deposition of the Ndembera Group. Above the nonconformity the basal quartzitic portions of Ndembera Group display only brittle behaviour, i.e. brittle fault planes and associated slickenside striations with east-over-west transport developed as shown in the summarizing sketch in Fig. 2f.

*4.1.3. Basement–granitoids relationship (Mloa)*

Paleoproterozoic retrogression and shear were partly accompanied by the emplacement of granitoids as exemplarily shown for Mloa (Figs. 1b, 2g–j). Here the W–E trending shear zone (Fig. 2h) exhibits dextral shear at greenschist to amphibolite facies conditions. Mafic magmatic enclaves (diorite xenoliths) frequently occur in the Usagaran granitoids (Fig. 2i). In places, melts intrude a network of joined shear and tension fabrics thereby disaggregating the host. In addition to above described shear sense indicators en-echelon oriented tension gashes and extensional shear zones (ecc fabrics) developed during deformation phase 2 in this outcrop (Fig. 2j). Granitoids and pegmatites intruded preferentially these sites of tension. Besides this late-syntectonic granitoid a variety of deformed and undeformed magmatic bodies dated around 1.8–1.9 Ma intruded the basement (Wendt et al., 1972). These multiple intrusions record a wide range of structures and display different magmatic pulses during progressive shear.

*4.1.4. Undeformed cover (Magalilwa)*

After cessation of deformation phase 2 the Magalilwa Group was deposited. The exact age of sedimentation of the Magalilwa Group is unknown but these sediments do not show any features of Paleoproterozoic deformation. The main rock types are coarse grained quartzitic conglomerates and quartzitic sandstones showing original sediment structures, e.g. cross-bedding. The conglomerates contain re-deposited sandstones and micro-conglomerates indicating at least one cycle of erosion and sediment reworking during or after the Usagaran orogenic cycle.

*4.2. Microtextural analysis*

In order to characterize the kinematics, flow geometry and approximate temperature regime during shearing, we sampled Qtz-bearing mylonites from the CTSB for a study on lattice preferred orientation (LPO). Especially the quartz-rich samples of the Usagaran Belt were suitable for LPO analysis.

*4.2.1. Basement (around Iringa)*

In thin section quartz is located interstitially between recrystallized feldspar (Fig. 3a). Deformation mechanisms lead to diffusion patterns with straight contact along migrating grain boundaries of quartz. In the non-migmatic basement gneisses K-feldspar is deformed by subgrain rotation (SR) deformation mechanism, quartz formed ribbons with grain boundary migration (GBM) mechanism (Fig. 3b). Within the Usagaran Basement high temperature deformed migmatites and basement gneisses preserved ribbon type quartz deformed under GBM and diffusion regimes. Typical for the samples along the CTSB are *c*-axes cross-girdle distributions corresponding to coaxial flow (Fig. 3c and corresponding thin section Fig. 3d). High opening angles $\alpha$ above 120° are interpreted as hint for high temperature at deformation phase 1. These pattern types are typically found in rocks deformed at granulite facies deformation (e.g. Fritz et al., 1996). The geometry of associated $\langle a \rangle$-axes is less-distinctive in this representative sample.

*4.2.2. Basement–cover relationship (Python Point)*

LPO patterns from samples just below the nonconformity to the Usagaran Ndembera volcano–sedimentary cover (outcrop Python Point) display asymmetric girdle distribution ($\beta = 29°$) compatible with dextral shear (Fig. 3e). Quartz *c*-axes patterns display prism $\langle a \rangle$, rhomb $\langle a \rangle$ and some basal $\langle a \rangle$ glide. We interpret this as progressive cooling from amphibolite to greenschist facies conditions that developed during deformation phase 2, when the Usagaran Basement was exhumed. Remnants of higher grade deformation are still preserved as prism $\langle a \rangle$ glide in the LPO pattern, lower grade deformation contributes to basal $\langle a \rangle$ glide. In thin section successive stages during retrogression are also documented from variable deformation mechanisms in quartz and feldspar. High temperature shear is supported from dynamically recrystallized feldspar with core-mantle structures (SR) and quartz deformed within the GBM regime. During cooling quartz grains were deformed by SR and BG with strongly elongated grains (Fig. 3f). Lower grade deformation stages are also indicated by saussuritisation of brittle feldspar. Finally, chlorite coated tension gashes and shear planes evolved at near surface conditions. The individual quartz grains of the basal quartzites above the nonconformity exhibit grain size reduction by fracturing and solution precipitation processes (Fig. 3g). Within the tuffs of the Ndembera group magmatic minerals are well preserved, the only deformation features are strain caps of sericite around

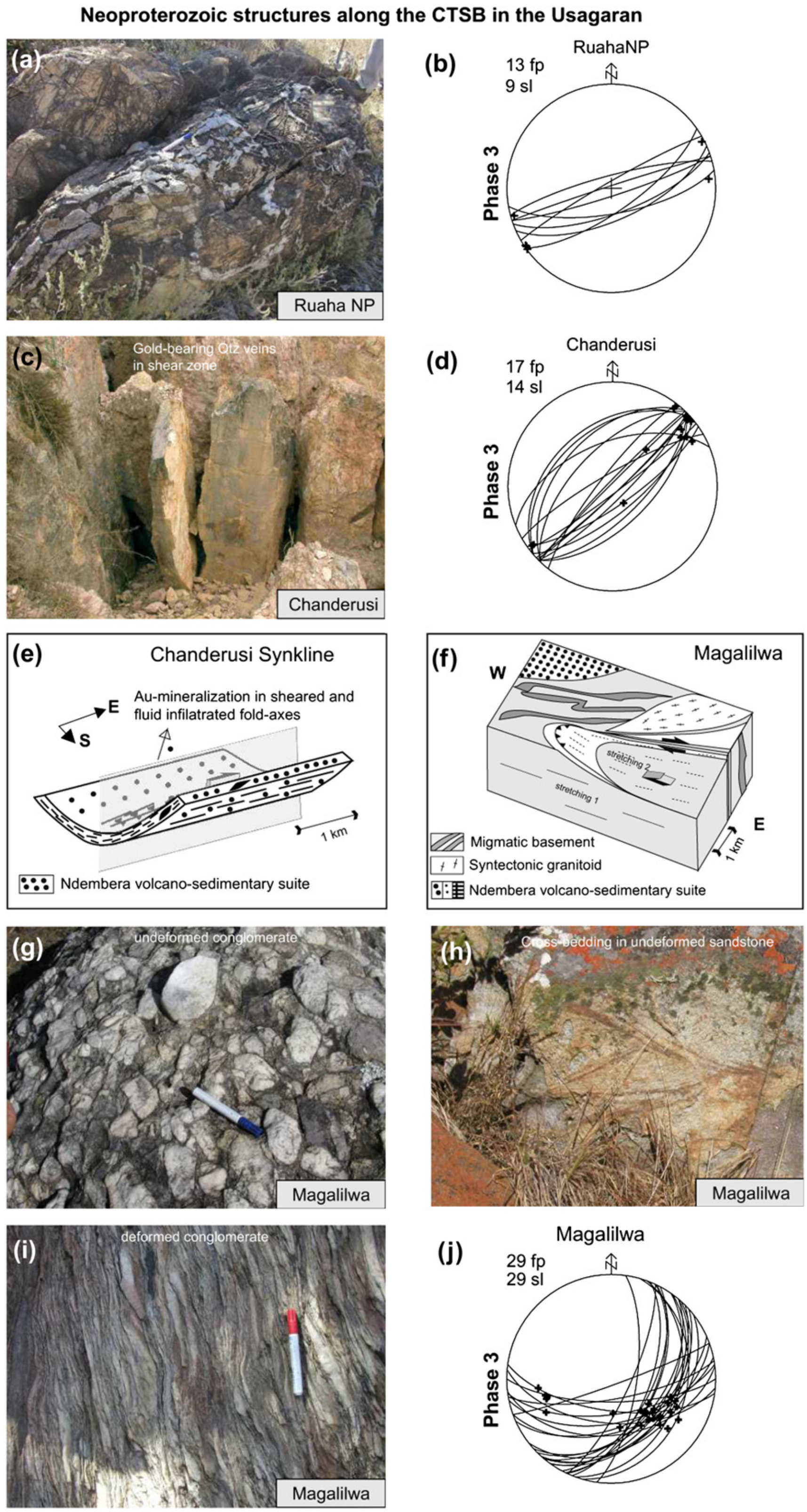


Fig. 4. Photomicrographs from thin sections with typical microstructures and mineral assemblages of the key areas for Neoproterozoic CTSB features in the Usagaran Belt. (a) Along the southern margin of the Tanzania Craton highly fluid infiltrated rocks (quartzites and marbles of the Konse Group) are typical. (b) The corresponding fabric elements from the Ruaha NP key outcrop. (c) The Chanderusi synform exhibits gold-bearing veins in highly sheared domains in the centre of the synform core. The photo shows a small deposit with steeply dipping foliation planes that is mined for gold. (d) The structural data for the Chanderusi synform show a NE−SW oriented fold pattern. (e) Schematic diagram summarizing the structural elements of Chanderusi. (f) One of the most spectacular localities of Paleoproterozoic sediments showing Neoproterozoic deformation is Magalilwa. The schematic diagram shows that Magalilwa exposes westward nappe sequences. The undeformed sediments occur in the core of the Magalilwa structure and are dominated by (g) coarse conglomerates, which contain partly reworked pebbles or (h) quartzitic units with sandstones containing ripple marks. (i) Various strain intensities are seen in the Magalilwa sediments depending on the position of sediments in the restraining bend. Extremely elongated conglomerate pebbles are found in the northern strike slip zone of the structure. (j) The structural inventory (top to the west thrusts and W−E trending strike slip zones) is seen in the plot with foliation planes and stretching lineation.

porphyroclasts and very mildly developed pressure seams coated with sericite (Fig. 3h).

Along the CTSB in the Usagaran Belt only Paleoproterozoic K/Ar mineral ages have been reported (Wendt et al., 1972). The microstructures from samples below the nonconformity reflect syndeformational temperature conditions above the Ar-retention temperature of ca. 400 °C. Thus all above described LPO patterns are interpreted to have evolved during Paleoproterozoic tectonic events.

#### 4.2.3. Basement–granitoids relationship (Mloa)

Some of the Usagaran granitoids preserved high temperature solid state deformation with dynamic recrystallization of feldspar and disc shaped quartz deformed at grain boundary migration regime – similar to those shown in Fig. 3a, b. In others the primary magmatic fabric is still preserved, feldspar shows saussuritisation and quartz deformed by SR at low strain. Undeformed granitoids exhibit clearly magmatic fabrics without hints for solid state deformation.

### 4.3. Summary of Paleoproterozoic tectonics along the CTSB

The CTSB in the Usagaran Belt is dominated by steep foliation and subhorizontal stretching as result of non-coaxial flow at various conditions. No arguments for Paleoproterozoic thrust tectonics have been observed. Paleoproterozoic tectonics along the CTSB in the Usagaran can be subdivided into two deformational phases. The CTSB exhibits high temperature distributed dextral shear that evolved during early tectonic activity (phase 1). This phase was characterized by vast migmatisation and intrusion of early granitoids. Strain was generally low during this phase. Simultaneously with cooling and exhumation of rocks close to surface, shear localized into distinct W–E trending mylonite zones evolved at amphibolite to greenschist metamorphic conditions and higher strain (phase 2). Weakly deformed granitoids intruded extensional sites of these shear zones. After rock exhumation to surface a phase of sedimentation is documented by deposition of the Ndembera volcano–sedimentary group and the Magalilwa Group. These sediments were delivered from the eroded basement. The final exhumation occurred probably simultaneous with sedimentation as indicated by redeposited Paleoproterozoic conglomerates and sandstones. Coevally with sedimentation late tectonic undeformed granitoids penetrated the crust.

## 5. Neoproterozoic tectonics along the CTSB

Neoproterozoic tectonics affected both the Usagaran and the Mozambique belts during a third deformational phase that reactivated the CTSB. Syntectonic metamorphic conditions increase eastwards along the CTSB with brittle to greenschist metamorphic conditions within the Usagaran Belt, increasing to upper amphibolite/granulite metamorphic conditions within the Mozambique Belt. We first describe the structural and metamorphic assemblies formed by the Neoproterozoic reactivation of the CTSB in the Usagaran Belt.

### 5.1. Neoproterozoic tectonics along the CTSB in the Usagaran Belt

#### 5.1.1. Field observations and macrostructures

The Neoproterozoic deformation in the Usagaran Belt is partitioned into strike slip zones and associated thrusts. Strike slip is localized mainly along the W–E trending margin of the Tanzanian Craton (along the Konse Group) and in fluid infiltrated shear zones within the Ndembera Group (Chanderusi) (Fig. 1c). Localized thrusts are best developed in the sedimentary units of the Magalilwa Group.

The main W–E trending strike slip fault is located immediately along the southern Craton margin. For example, in the Ruaha National Park (Fig. 1c) intense solution–precipitation processes formed rocks that partly contain up to 50% quartz and carbonate veins (Fig. 4a). These gneisses are heavily retrogressed during fluid assisted shear. Feldspar is almost entirely replaced by sericite, epidote and chlorite indicating deformation at greenschist facies conditions.

Where the Craton margin bends north this fault cuts the Usagaran Belt north of Iringa and continues to the Mozambique Belt. Parallel to the main fault system some W–E trending faults developed south of Iringa (Fig. 1c). Between these W–E trending fault zones, NE–SW trending faults and folds developed that incorporate slices of Ndembera volcanics. One of these Ndembera shear slices, here referred as Chanderusi synform (Fig. 1c), is a NE–SW trending fold structure with an associated dextral, NE–SW trending shear zone in the synform core (Fig. 4c–e). Shearing and fluid infiltration gave rise to a small vein type ore deposit with mobilisation of sulphide and gold from the volcanics and precipitation within the fault zone (Fig. 4c). Besides the strike slip tectonics some fault plane solution data gave horizontal NW–SE oriented maximum principal stresses and subvertical minimum principal stresses suggesting the presence of local thrusts. An example for a thrust regime associated with general strike slip deformation is found in Magalilwa. In Magalilwa (Fig. 4f) the only map scale east-over-west thrust is exposed along the CTSB. The eastward dipping thrust juxtaposes partly undeformed conglomerates, quartzitic sandstones and schists of Usagaran cover onto the migmatic basement (Fig. 4g, h). The thrust is bending northwards into a W–E striking steep shear zone which is part of the CTSB (Fig. 4f, j). Significant strain heterogeneities occur in Magalilwa as shown by the conglomerates (Fig. 4g, i). The frontal part of the thrust exhibits low W–E stretch as seen from sheared pebbles seamed by shear bands of muscovite. Approaching the northern shear zone strain intensity becomes much higher and sedimentary bedding steepens here defining the high strain northern dextral shear zone. This thrust is interpreted as a restraining bend between dextral shear zones.

#### 5.1.2. Microtextural analysis

Along the Southern Craton margin low-grade strike slip deformation associated with fluid flow goes along with quartz $c$-axes patterns showing basal $\langle a \rangle$ glide (peripheral maxima) and a flow geometry close to simple shear (pronounced external asymmetry of peripheral ⟨a⟩-axes) (Fig. 5). Some remnants of older, higher grade deformation may be preserved in a relic prism ⟨a⟩ glide pattern. The kinematics derived from the external asymmetry is clearly dextral (Fig. 5a, c). It should be mentioned that ductile quartz fabrics are later overprinted by brittle dextral shear planes. Microstructures in both, the Ruaha NP and the Chanderusi area, are dominated by SR in Qtz (Fig. 5b, d). Pressure solution and precipitation can be commonly observed as well as widespread saussuritisation of feldspar.

At the ridges of the Magalilwa hill LPO patterns show a transition from east-over-west thrust geometry in the west to dextral strike slip geometry in the north (Fig. 6a–e). This geometry is best described as restraining bend during westward displacement of nappes. The following observations can be made from LPO patterns shown in Fig. 6a–e.

(1) The asymmetry of *c*-axes indicates east-over-west shear deformation along the western thrust (Fig. 6a, b) and dextral strike slip deformation in the northern high strain zone (Fig. 6c–e). All ⟨a⟩-axes are single maxima oblique to the foliation which again supports non-coaxial flow during top to the west or dextral shear. This is consistent with shear sense indicators observed in the field and in thin sections.
(2) In all cases ⟨a⟩-axes are distributed along the periphery of the stereonet indicating plane strain.
(3) Quartz *c*-axes patterns show dominantly single girdle distributions oblique to the foliation. There is only a weak tendency to evolve cross-girdles as seen from subordinately developed legs in the internal asymmetry. This again suggests dominance of non-coaxial flow.
(4) The *c*-axes patterns suggest simultaneous activity of three glide planes. Prism ⟨a⟩ glide is seen in maxima around the *Y*-axes, rhomb ⟨a⟩ glide to maxima between the centre (*Y*) and periphery of the stereonet and basal ⟨a⟩ to peripheral maxima.

Magalilwa is an excellent example for the contiguity between the thrusting and strike slip regimes of deformational phase 3. Together with changing kinematics we observed a strong strain gradient with mildly deformed pebbles along the western thrust ($Rf < 2$) over strained pebbles with $2 < Rf < 5$ in the transition zone between thrust and strike slip domain and very high strained pebbles ($Rf > 10$) along the northern strike slip zone (Fig. 4g, i).

The accessibility of strain data allows a detailed study on texture evolution and vorticity. For steady-state plane strain isochoric deformation, the mean vorticity ($W_m$) is a function of the angle $\beta$ and the finite strain (Rf) (Wallis, 1992; Grasemann et al., 1999). In Magalilwa strain is recorded in quartz pebbles that have been analysed together with lattice preferred orientation patterns. Almost independent of strain magnitude the central segment of quartz *c*-axes occupies angles between 15° and 23° to the trace of the foliation. When strain data and $\beta$-angles are plotted (Fig. 6f; for analytical details see Grasemann et al., 1999), a clear trend is seen from simple shear dominated flow ($W_m$ close to 1) in the northern high strain strike slip domain towards enhanced contribution of pure shear component ($W_m = 0.4–0.6$) within the western thrust domain. One example within the western thrust domain (Fig. 6c) has a low $\beta$-angle of 8°. This goes along with more pronounced cross-girdle distribution compared to the other samples and

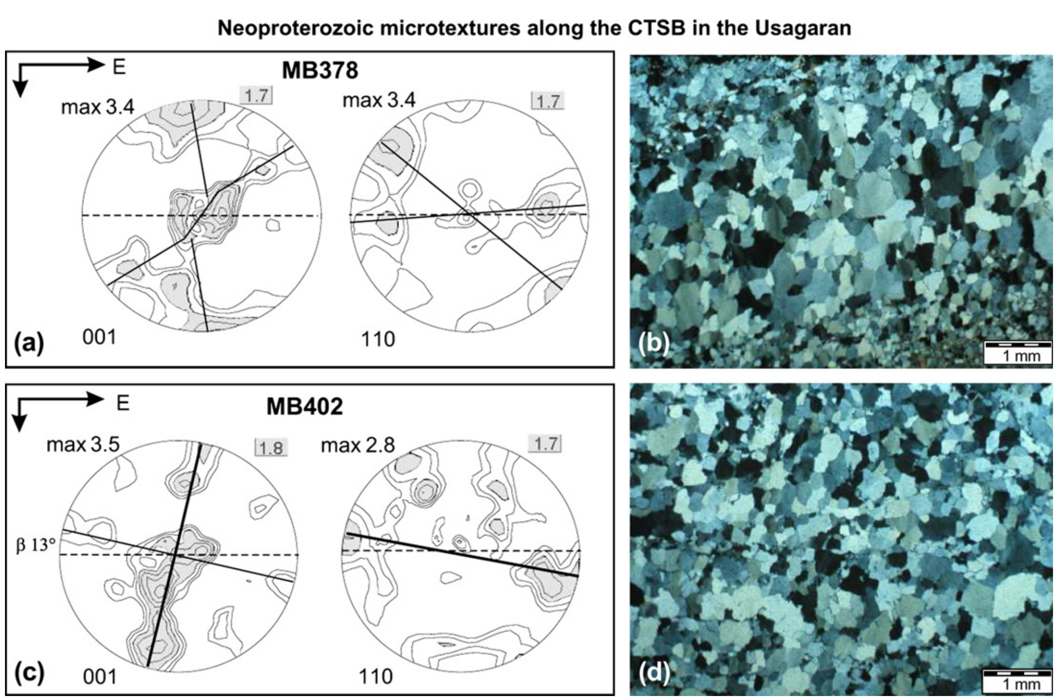


Fig. 5. Pole figures of LPO of quartz (⟨c⟩- and corresponding ⟨a⟩-axes) for Neoproterozoic deformational phases found along the CTSB in the Usagaran. Thin sections of the quartz fabric for the samples are added. MB378 and MB402: Craton Margin in the Ruaha National Park.

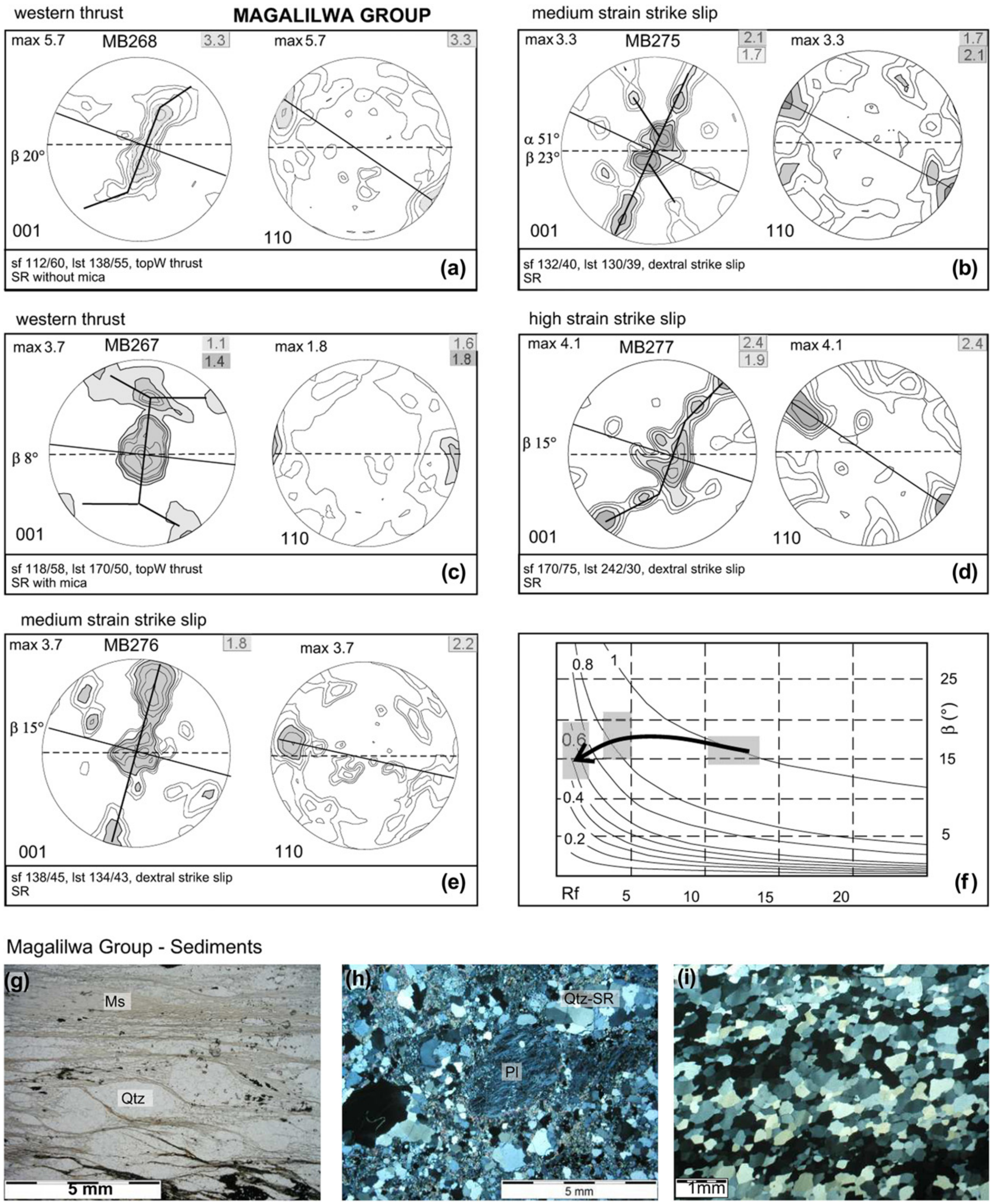


Fig. 6. An example for the Neoproterozoic strain gradient in the CTSB is well preserved in the Paleoproterozoic sediments of the Magalilwa Group. (a–e) From thrust (upper left) to strike slip (lower right) and from low strain (R:3) to high strain (R:15). (f) Rf − $\beta$ diagram (after Grasemann et al., 1999) showing the increase of vorticity from strike slip to thrust geometry. (g–i) Representative photomicrographs for Magalilwa. (g) A micaceous sandstone from the Magalilwa Group that was mildly metamorphosed with s–c fabrics defined by asymmetric Qtz grains with Ms in between. Displacement is top W in this thin section. (h) An argument for the precursor rocks from the Magalilwa sediments is shown in this section. Central portions of Magalilwa contain coarse grained sandstones with relics of Pl indicating that the Usagaran granitoids might have contributed to these sediments. (i) The typical deformation mechanism of Qtz in these rocks is subgrain rotation (SR).

also supports a higher contribution of non-coaxial flow along the western thrust domain.

We supplemented three thin sections from the Magalilwa samples (Fig. 6g–i). Fig. 6g shows a micaceous sandstone that was mildly metamorphosed with an s–c fabric defined by asymmetric Qtz grains with Ms in between. Displacement is top W in this thin section. Wendt et al. (1972) dated white mica from a sericite phyllite and received pre-Neoproterozoic white mica ages for the Rb/Sr System (1283 ± 35 Ma) and Neoproterozoic ages (515–550 Ma) for the K/Ar System. This suggests temperature conditions below the closure temperature of white mica of ca. 500 °C and above the Ar-retention temperature of 400 °C for the deformation (McDougall and Harrison, 1988; Paquette et al., 1989) and allows the assumption of a Neoproterozoic deformation age in Magalilwa.

Fig. 6h shows that in some coarse grained sandstones remnants of altered magmatic plagioclase can be found that suggest the erosion of an igneous source, probably the magmatic Usagaran Basement.

The quartz patterns have evolved at upper greenschist metamorphic conditions, which is in concordance with dominant SR mechanism in quartz and with geochronological data (Fig. 6i).

### *5.2. Neoproterozoic tectonics along the CTSB in the Mozambique Belt*

The CTSB in the Mozambique Belt is less accessible compared to the Usagaran Belt, because of several difficulties. Firstly, large parts of the shear belt are located in the Udzungwa Mountains National Park which is a forest reserve. Secondly, no good geological maps are available and thirdly, shear is distributed over tens of kilometres and no distinct localized shear zone can be defined. The main Neoproterozoic CTSB is traced from Ilula eastwards. It roughly follows the Lukozi River and continues across the Udzungwa Mountains to the Ruaha River valley until Kidatu (Fig. 1c). Within the Kilombero Valley the CTSB is cut discontinuously by the Phanerozoic Karoo rift sediments (Nilsen et al., 2001). Further east the Ruaha River cuts the Eastern Granulites and follows a W–E oriented shear zone into areas that have not been studied at all (hardly accessible parts of the Selous Game Reserve). Nevertheless, CTSB structures are found along several road cuts along the Lukozi and Ruaha river valleys west of Mikumi and along the road to Kidatu power plant (Fig. 1c). From these road cuts the following key outcrops are discussed.

#### *5.2.1. Field observations and macrostructures*

The structural inventory of the Mozambique Belt differs significantly from the Usagaran Belt (Fritz et al., 2005; Vogt et al., 2006). North of the CTSB top to the west fold and thrust tectonics is characteristic, whereas south of the CTSB W–E trending steep shear zones dominate. Fritz et al. (2005) defined the CTSB as a boundary shear zone separating the northern and southern tectonic domains. In the Western Granulites the CTSB is a ductile mylonite zone with a bundle of parallel shear zones (Fig. 1c). In domains between shear zones W–E stretch and folding with W–E fold axes are observed. The boundary between the Usagaran and the Mozambique Belt shows a complex pattern of thrusts and associated shear zones. The combination of Neoproterozoic thrusts and strike slip shear zones formed a staircase pattern along this margin (Fig. 1a). This geometry can be explained as restraining bends between strike slip zones, in a larger scale similar to the situation at Magalilwa.

Whereas the kinematics of the CTSB within in the Usagaran Belt is dextral simple shear, the flow geometry in the Western Granulites is pure shear dominated with less distinct shear sense indicators. From map scale and dominant structures a major dextral sense of shear can be inferred. The CTSB in the Western Granulites is of Neoproterozoic age and exhibits a strong temperature gradient ranging from greenschist facies conditions in the west up to granulite facies conditions in the east (Fig. 7).

Close to the boundary between Usagaran and Mozambique Belts semi-ductile fabrics occur in the area around Iringa (Fig. 7a). Along this structural boundary the trace of the CTSB is disaggregated into various zones of complex geometry formed by the partitioning of deformation into thrusts and strike slip zones. In the westernmost part of the Western Granulites next to Ilula foliation planes trend NE (Fig. 7b) but also NW trending vertical zones can be found. Fabric elements in this key area are complex, to some extent, because of the deflection around a rigid Paleoproterozoic pluton (Fig. 1c). Another example for the influence of the CTSB is shown in the location Ruaha River (Figs. 1c, 7c). The migmatic gneisses of the Ruaha River road cut show top to the NW asymmetric folds that are slightly stretched in NE–SW direction (Fig. 7d). Additionally, foliation planes are slightly folded and stretched into W–E direction. Approaching the CTSB the NE trend turns into a W–E orientation. Northwards of the CTSB the NE trend turns into a N–S direction representing Pan-African thrusts of the Western Granulites north of the Ruaha River (Fig. 1c). Within the Lukozi River area HT shear and localized melt fabrics occur (Fig. 7e). Also dextral shear sense is inferred from asymmetric folds in the Lukozi area. The road to Kidatu power plant exhibits the CTSB as a clearly W–E trending zone of stretched folds in outcrop scale but also in a regional scale as shown in Fig. 7g, h. The granulites and migmatic gneisses of Kidatu exhibit some flat-lying fold limbs (Fig. 7h). However, the majority of fold limbs and strike slip zones is steeply dipping N with dextral shear sense indicators (deformed feldspar clasts).

#### *5.2.2. Microtextural analysis*

Within the CTSB in the Mozambique Belt conditions grade from amphibolite facies along the boundary between Usagaran to Mozambique Belt to upper amphibolite/granulite facies further east. Quartz LPO patterns reflect this scenario. Close to the Usagaran Mozambique boundary (Ilula) quartz *c*-axes show a combination of basal $\langle a \rangle$, rhomb $\langle a \rangle$ and prism $\langle a \rangle$ glide (Fig. 8a). *c*-Axes display slightly asymmetric cross-girdle distribution with a moderate opening angle of

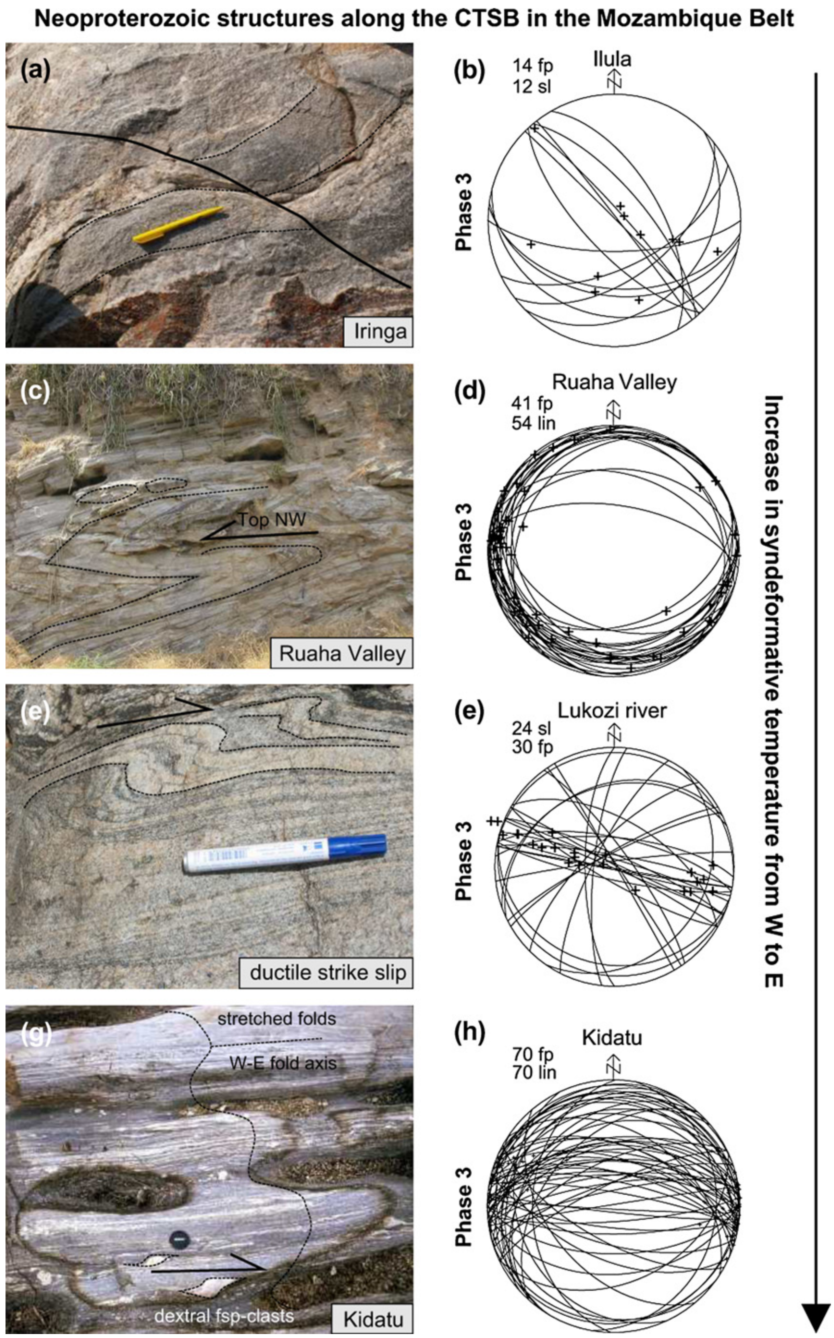


Fig. 7. Representative outcrop photographs and structural data from locations, where the Neoproterozoic tectonics along the CTSB in the Mozambique Belt is seen. (a) This example is from the area around Iringa (close to the boundary to the Mozambique Belt) where semi-ductile fabrics can be associated with the Neoproterozoic overprint of the pre-existing highly ductile Usagaran fabric. (b) Further east the structural imprint is shown from Ilula. (c) Towards the Ruaha River section the degree of metamorphic grade increases in the Western Granulites eastwards and the structures are slightly stretched into W–E orientation. (d) A shear zone in the westernmost portions of the Western Granulites (Lukozi River) shows indicators for dextral shear – e.g. sheared migmatic folds. (f) The corresponding structural plot for this outcrop. (g) Stretched fold limbs in dm-scale with dextral shear sense are found in Kidatu. (h) The folding with development of steeply oriented northwards dipping shear zones is represented by the foliation planes and lineation from Kidatu.

$\alpha = 95°$ between peripheral legs. Quartz $\langle a \rangle$-axes show two maxima asymmetrically arranged around *X*. This indicates a contribution of non-coaxial flow. The kinematics of this sample suggests oblique thrusting of Mozambique onto Usagaran units. Deformation mechanisms in quartz are SR and GBM (Fig. 8b). *c*-Axes patterns within the Ruaha valley display typical granulite facies patterns (Fig. 8c, d) with symmetric cross-girdle distribution and extremely high opening angle $\alpha$ (105°). Here quartz *c*-axes have been measured by U-stage technique. In thin sections the Neoproterozoic fabrics show diffusion patterns in quartz with disc shape and GBM of feldspar (Fig. 8d). This deformation regime continues along the Ruaha River valley to the easternmost outcrops at Kidatu.

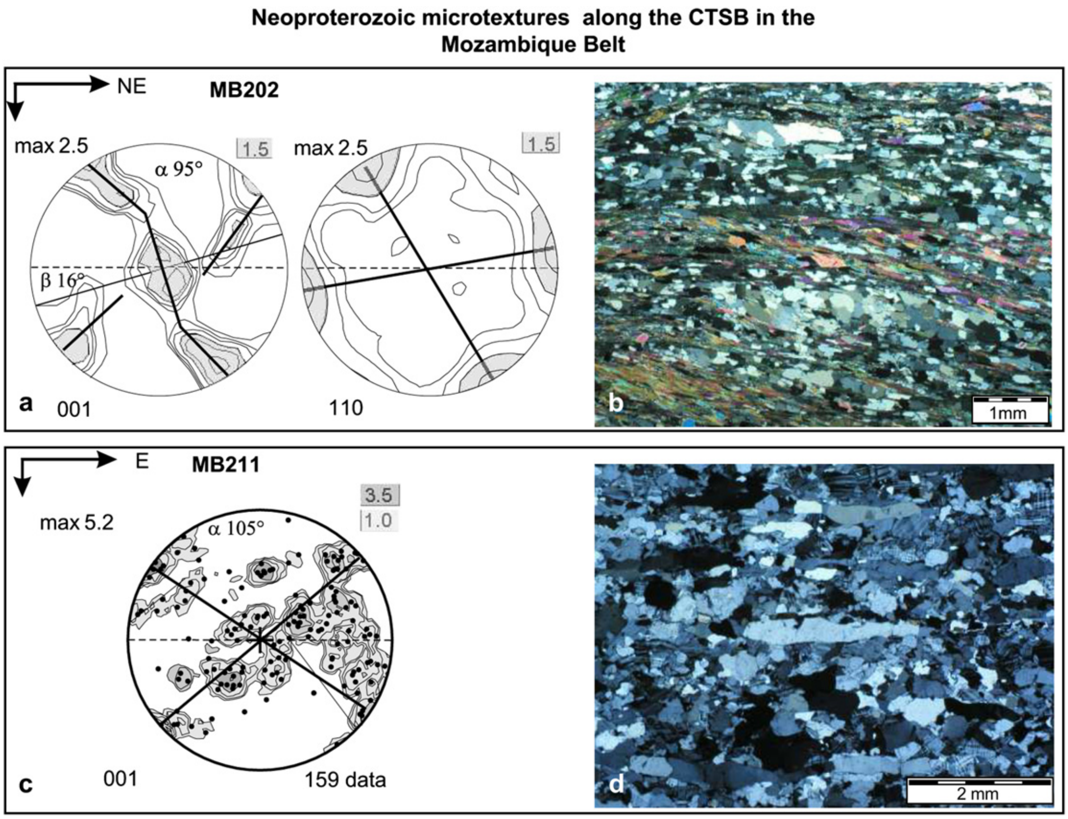


Fig. 8. Pole figures of LPO of quartz (⟨c⟩- and corresponding ⟨a⟩-axes) for Neoproterozoic deformational phases found along the CTSB in the Mozambique Belt. MB211, Ruaha valley; MB202, Ilula.

### 5.2.3. Summary of Neoproterozoic tectonics along the CTSB

The Paleoproterozoic CTSB has been reactivated by a deformational phase in the Neoproterozoic (phase 3). The boundary between Mozambique and Usagaran Belts is generally dominated by a combination of thrusting and strike slip along the CTSB. This is in contrast to predominately strike slip tectonics in the Paleoproterozoic. A gradient in syntectonic metamorphism from west to east from greenschist to granulite facies conditions is observed along the CTSB. West of Iringa faults and associated slickensides are dominant, close to Iringa first semi-ductile fabrics evolve and approaching the Mozambique Belt ductile fabrics become dominant. This is also reflected in the deformation mechanisms in quartz changing from BG over SR to GBM and diffusion processes. The structural observations in the Western Granulites indicate that shear was accompanied by dominant W–E stretch that re-orientated the previously formed fabric. Fold axes rotated towards the stretching direction and shear zones developed along steep fold limbs grading into dextral strike slip zones.

## 6. Discussion

### 6.1. General implications from LPO patterns

Models suggest temperature dependence of preferentially active glide systems in quartz. Our study shows a good agreement between temperatures derived from LPO with temperatures derived from deformation mechanisms (Stipp et al., 2002). Basal ⟨a⟩ glide has been found in elongated quartz grains with bulging mechanism, rhomb ⟨a⟩ glide typifies the SR and GBM mechanisms. Prism ⟨a⟩ glide has been found in ribbon quartz with dominantly GBM and diffusion.

It has also been proposed that, in coaxial flow, a temperature increase leads to an increase of the opening angle $\alpha$. Together with the increase of the opening angle $\alpha$, the angle $\beta$ decreases systematically in our stereo plots. From west to east along the Neoproterozoic CTSB the angle $\alpha$ increases from 55° (Usagaran) over 95° (Usagaran/Mozambique Belt boundary) to 108° (Western Granulites) and the angle $\beta$ decreases from 23° over 16° to almost 0° (Fig. 9a–c). An increase of the opening angle $\alpha$ and a decrease of the angle $\beta$ go along with a decrease of vorticity with rising temperatures. This vorticity decrease from around 1 (simple shear) to 0 (pure shear) is shown in Fig. 9d. Required strain (Rf) data were not available so we roughly assumed a strain variation between $Rf = 5$ and 8 to qualitatively distinguish between pure shear and simple shear dominated domains. Temperature variation obviously influences shear localization as we found localized non-coaxial shear in the western low temperature domain and highly distributed coaxial shear in the eastern high temperature CTSB.

### 6.2. The role of the Tanzania Craton for the CTSB

The shape of the Tanzania Craton played a major role in the formation of both the Neoproterozoic and Paleoproterozoic shear belts defining the long-lived CTSB. The indenter

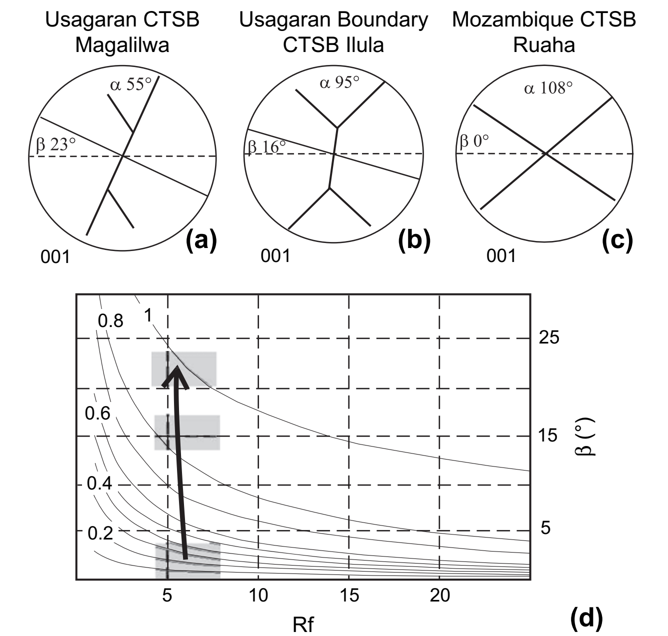


Fig. 9. Idealized sketches with skeletons of LPO quartz patterns derived from the typical samples along the CTSB. (a–c) Evolutionary trends in syndeformative temperature derived from LPO patterns of quartz following the methods of Kruhl (1996) and Law et al. (2004). (c) Vorticity analysis using LPO texture of quartz using a diagram Rf versus b (after Grasemann et al., 1999).

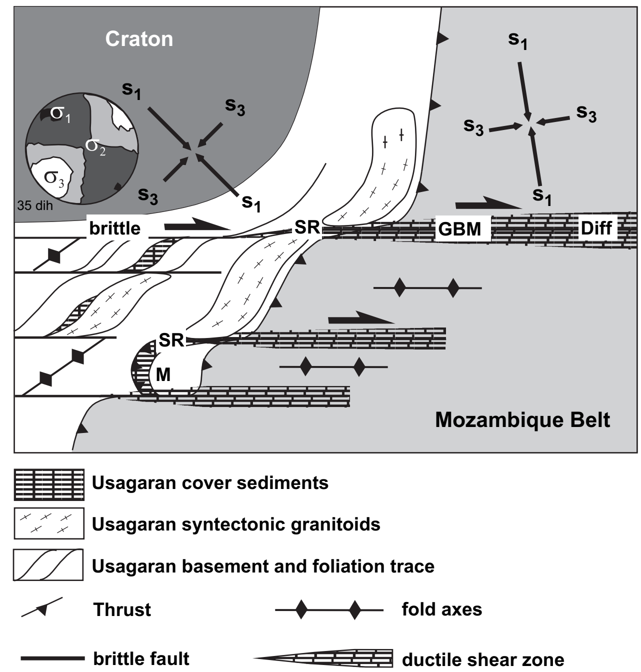


Fig. 10. The geometry of the Neoproterozoic CTSB in map view showing changes in tectonic features (temperature, stress field, structural elements) from the Usagaran in the west towards the Mozambique Belt in the east.

geometry of the rigid Tanzania Craton controlled shear localization parallel and along the southern W–E trending Craton margin. In the entire Usagaran CTSB NNW–SSE trending subvertical quartz tension gashes are compatible with dextral shear. Some older pegmatite veins with NW–SE to W–E orientation have been synthetically rotated during Neoproterozoic shear (Fig. 10). Fault plane solution data show dextral strike slip with NW–SE oriented maximum principal stress axes and NE–SW minimum principal stress axes (Fig. 10).

Oblique Paleoproterozoic island arc accretion released in tensional structures at low stress segments around the Craton giving space to magma emplacement. Therefore much of the Paleoproterozoic deformation in the Usagaran was achieved by melt enhanced deformation. Strike slip zones are vastly invaded by syntectonic granitoids. Large portions of the granitoids display magmatic flow without hints for solid state deformation. Low strain volume diffusion type deformation and coaxial flow suggest distributed shear in softened crust. This contrasts the Neoproterozoic deformation that occurred only at solid state conditions in a mechanically stronger crust. The Neoproterozoic CTSB is interpreted as a release structure (counterflow shear zone after Talbot, 1999) that evolved during overall crustal thickening in the stress shadow of the indenting Tanzania Craton. This counterflow shear zone penetrated the upper crust in the west (Craton margin) and extends to the crust/mantle boundary in the eastern orogen root zone. A metamorphic gradient with widely different textures is preserved along the CTSB from W to E. This goes along with a different style of shear zones. Localized non-coaxial shear (plane strain) occurs at upper crustal low temperature deformation and distributed coaxial shear occurs at lower crustal high temperature deformation (three-dimensional deformation). The CTSB provides an excellent example where shear deformation may be traced over some hundreds of kilometres with changing rheology and crustal penetration depth along strike.

### 6.3. Exhumation histories along the CTSB

Two periods of exhumation can be distinguished along the CTSB. A Paleoproterozoic exhumation phase up to the surface is related to distributed wrench tectonics. There is not much known about the exhumation history that brought the Usagaran Basement to the surface. Amphibolite facies rocks had to be brought to the surface during the Paleoproterozoic before onset of Ndembera and Magalilwa sedimentation. At final exhumation stages the amount of exhumation was low as indicated by shallow level plutons. Hence the Paleoproterozoic sediments that were deposited in the course of rock exhumation might still be preserved nearby the denudation centre. This contrasts the Neoproterozoic exhumation that is mainly related to thrust tectonics which exposed, in the eastern units, high-pressure granulites close to the surface (Fritz et al., 2005). When exhumation is balanced by erosion, the erosion rates must have been high in the Neoproterozoic and large volumes of sediments have been removed. This might explain why Neoproterozoic molasse sediments are largely absent within the Mozambique Belt.

### 6.4. General regional implications for the two Proterozoic belts

The two Proterozoic orogenic belts can be distinguished on the basis of several criteria.

(1) Since the studies of Wendt et al. (1972) the rough geometry of the boundary between two belts is known from the distribution of metamorphic age groups that document a Neoproterozoic, Pan-African thermal front overprinting rocks with Paleoproterozoic ages.
(2) Another criterion is the extreme difference in the tectonic style. The structures of the Usagaran Belt are characterized by strike slip zones with vertical foliation planes. The Mozambique Belt, in contrast, is best described as top to the west thrust and fold belt with generally flat-lying foliation transposed by the W–E trending CTSB.
(3) Tectonic transport of units in the Usagaran is limited to strike slip shear with little displacement. There is no indication of a spatial metamorphic gradient in the HT basement of the study area. By contrast, the Mozambique Belt exposes a metamorphic gradient from western lower amphibolite facies to eastern granulite facies. This gradient arose from nappe transport along deepening decollement levels over many kilometres onto the Tanzanian Craton and the pre-existing Usagaran Belt (Fritz et al., 2005).
(4) In the southern Usagaran large volumes of syn- to post-deformational intrusive rocks were emplaced coeval with strike slip tectonics. This is in strong contrast to the Mozambique Belt where mainly highly deformed and metamorphosed rocks occur.

Daly (1988) has outlined in a kinematic study on the Ubendian Belt that much of Proterozoic plate tectonics is characterized by horizontal displacements. Based on a study of Shackleton and Ries (1984) on kinematics of the Usagaran Belt, Daly (1988) argued that the Ubendian tectonics resolved in the formation of vertical shear zones between different terranes along the Tanzania Craton whereas coevally the Usagaran Belt was formed by thrusting onto the Tanzania Craton. Our study agrees with the idea of Daly (1988) that Paleoproterozoic tectonics (Usagaran and Ubendian systems) is characterized by the formation of steep shear zones around or between Archean Cratons. However, we do not agree with Usagaran thrust tectonics as the majority of Usagaran structures is vertically oriented. Some minor thrusts have been found, however, these can be related to the Neoproterozoic overprint along the CTSB by localized thrusts (e.g. Magalilwa Group).

All these differences show that there are major differences in the tectonic evolution of both belts and plate tectonics did not remain uniform during the whole Proterozoic.

## 7. Conclusions

The CTSB is considered as wrench zone where shear was initially localized along the stiff Tanzanian Craton during the Paleoproterozoic and subsequently reactivated during the Neoproterozoic orogeny. The deformational events within the CTSB can be subdivided into several phases.

Phase 1: Paleoproterozoic distributed HT shear in the Usagaran Basement:
A migmatic, NE trending foliation in the basement is the predominant structural feature indicating a HT-tectonometamorphic event. Quartz *c*-axes typify coaxial high temperature shear. Diffusion mechanisms in quartz point to high temperatures, strain and strain rate is considered low because in situ melts still form networks. The minimum age of this event is 1.9 Ga being older than Ndembera volcanics and Usagaran granitoids.

Phase 2: Paleoproterozoic exhumation:
The Usagaran Basement experienced exhumation before the deposition of the Ndembera volcanics. Exhumation was related to dextral strike slip tectonics along W–E trending shear planes. LPO patterns are typical for lower temperature deformation. Shape preferred quartz deformed by SR and bulging indicates retrogression down to greenschist facies conditions. Temperature decrease goes along with the documented increase of vorticity and strain. In some places granitoid melts with still preserved magmatic fabrics intruded the basement along the CTSB and enabled local melt enhanced deformation. The ca. 1.9 Ga age of exhumation is constrained by the subsequent sedimentation of the Ndembera Group.

The retrogressed sequences below the nonconformity indicate an exhumation phase before onset of the sedimentation of the Ndembera Group. This Paleoproterozoic exhumation phase can also be inferred from sediments of the Konse and Magalilwa Groups.

Phase 3: Neoproterozoic localized thrusting and strike slip in the Usagaran:
Localized, low temperature highly partitioned deformation is the common feature of Neoproterozoic tectonics in the Usagaran. (1) Bundles of discrete W–E trending brittle to ductile dextral strike slip faults define the CTSB. Associated is open NE–SW trending folding (Chanderusi synform) that postdates deposition of Ndembera volcanics. (2) Top to the west thrusts and associated dextral strike slip zones with a strong strain and vorticity gradient (Magalilwa) are interpreted as restraining bend between strike slip domains. The quartz LPO patterns are typically oblique single girdles. Deformation mechanisms include solution and precipitation processes in the west and SR in eastern high strain domains. At the boundary to the Mozambique Belt cross-girdles with moderate opening angles suggest deformation at elevated temperatures and a contribution of coaxial flow.

Phase 3: Neoproterozoic distributed strike slip in the Western Granulites of the Mozambique Belt:
Distributed high temperature dextral shear transposing thrusts characterizes the CTSB in the Western Granulites. The step-shaped Usagaran/Mozambique Belt boundary is a result of macro-scale restraining bends between strike slip domains. From the western Mozambique Belt boundary to the east an increase in temperature and increase of coaxiality can be observed. Dynamically recrystallized feldspars and disc quartz display very high temperature deformation in the east. This goes along with change from amphibolite to granulite facies deformation.

## Acknowledgements

We acknowledge the logistic and scientific support of E. Wallbrecher, S.M. Muhongo and C.K. Makene during our field studies in the CTSB. H. Sommer is thanked for discussions regarding the chronological and metamorphic history of the study area. For technical support we thank G. Zmugg. This study was enabled by funding from the Austrian Science Foundation (FWF Projects P15599 and T247-N10). We thank the reviewers S. Reddy and G. Viola for their helpful comments.

## References

Bunge, H.J., 1981. Fabric analyses by orientation distribution functions. Tectonophysics 78, 1–21.

Collins, A.S., Pisarevsky, S.A., 2005. Amalgating eastern Gondwana: The evolution of the Circum-Indian Orogens. Earth Science Reviews 71, 229–270.

Collins, A.S., Reddy, S.M., Buchan, C., Mruma, A., 2004. Temporal constraints on Palaeoproterozoic eclogite formation and exhumation (Usagaran Orogen, Tanzania). Earth and Planetary Science Letters 224, 175–192.

Daly, M.C., 1988. Crustal shear zones in central Africa: a kinematic approach to Proterozoic tectonics. Episodes 11, 5–11.

Fritz, H., Dallmeyer, R.D., Neubauer, F., 1996. Thick-skinned versus thin-skinned thrusting: rheology controlled thrust propagation in the Variscan collisional belt (the southeastern Bohemian Massif, Czech Republic – Austria). Tectonics 15, 1389–1413.

Fritz, H., Tenczer, V., Hauzenberger, C.A., Wallbrecher, E., Hoinkes, G., Muhongo, S., Mogessie, A., 2005. Central Tanzanian Tectonic Map (CTTM): a step forward to decipher Pre Pan-African and Pan-African structural events. Tectonics 24 (6), TC6013.

Grasemann, B., Fritz, H., Vannay, J.-C., 1999. Quantitative kinematic flow analysis from the Main Central Thrust Zone (NW-Himalaya, India): implications for a decelerating strain path and the extrusion of orogenic wedges. Journal of Structural Geology 21, 837–853.

Hepworth, J.V., 1972. The Mozambique Orogenic Belt and its foreland in northeast Tanzania: a photogeologically-based study. Journal of the Geological Society of London 128, 461–500.

Kröner, A., 1977. The Precambrian geotectonic evolution of Africa: plate accretion versus plate destruction. Precambrian Research 4, 163–213.

Kruhl, J.H., 1996. Prism- and basal-plane parallel subgrain boundaries in quartz: a microstructural geothermobarometer. Journal of Metamorphic Geology 14, 581–589.

Law, R.D., Schmid, S.M., Wheeler, J., 1990. Simple shear deformation and quartz crystallographic fabrics: a possible natural example from the Torridon area of NW Scotland. Journal of Structural Geology 12, 29–45.

Law, R.D., Searle, M.P., Simpson, R.L., 2004. Strain, deformation temperatures and vorticity of flow at the top of the Greater Himalayan Slab, Everest Massif, Tibet. Journal of the Geological Society 161, 305–320.

Lister, G.S., Williams, P.F., 1979. Fabric development in shear zones: theoretical controls and observed phenomena. Journal of Structural Geology 1, 283–297.

Lister, G.S., Hobbs, B.E., 1980. The simulation of fabric development during plastic deformation and its application to quartzite: the influence of deformation history. Journal of Structural Geology 2, 355–370.

Maboko, M.A.H., 2000. Nd and Sr isotopic investigation of the Archean-Proterozoic boundary in north eastern Tanzania: constraints on the nature of Neoproterozoic tectonics in the Mozambique belt. Precambrian Research 102, 87–98.

Maboko, M.A.H., Nakamura, E., 1996. Nd and Sr isotopic mapping of the Archaean–Proterozoic boundary in southeastern Tanzania using granites as probes for crustal growth. Precambrian Research 77, 105–115.

McDougall, I., Harrison, T.M., 1988. Geochronology and Thermochronology by the 40Ar/39Ar Method. Oxford University Press, New York, 212 pp.

Möller, A., Appel, P., Mezger, K., Schenk, V., 1995. Evidence for a 2 Ga subduction zone: eclogites in the Usagaran Belt of Tanzania. Geology 23, 1067–1070.

Möller, A., Mezger, K., Schenk, V., 2000. U–Pb dating of metamorphic minerals: Pan-African metamorphism and prolonged slow cooling of high pressure granulites in Tanzania, East Africa. Precambrian Research 104, 123–146.

Mruma, A., 1995. Stratigraphy and palaeodepositional environment of the Palaeoproterozoic volcano–sedimentary Konse Group in Tanzania. Journal of African Earth Sciences 21 (2), 281–290.

Muhongo, S., Kroener, A., Nemchin, A.A., 2001. Single zircon evaporation and SHRIMP ages for granulite facies rocks in the Mozambique Belt of Tanzania. The Journal of Geology 109, 171–189.

Nilsen, O., Hagen, E., Dypvik, H., 2001. Sediment provenance and Karoo rift basin evolution in the Kilombero Rift Valley, Tanzania. South African Journal of Geology 104, 137–150.

Paquette, J.-L., Chopin, C., Peucat, J.-J., 1989. U–Pb zircon, Rb–Sr, and Sm–Nd geochronology of high- to very high-pressure meta-acidic rocks from the western Alps. Contribution to Mineralogy and Petrology 101, 280–289.

Passchier, C.W., Trouw, R.A.J. (Eds.), 1996. Microtectonics. Springer-Verlag, Berlin/Heidelberg.

Platt, J.P., Behrmann, J.H., 1986. Structures and fabrics in a crustal-scale shear zone, Betic Cordillera, SE Spain. Journal of Structural Geology 8, 15–33.

Reddy, S.M., Collins, A.S., Mruma, A., 2003. Complex high-strain deformation in the Usagaran Orogen, Tanzania: structural setting of Palaeoproterozoic eclogites. Tectonophysics 375, 101–123.

Reddy, S.M., Collins, A.S., Buchan, A.C., Mruma, A.H., 2004. Heterogeneous excess argon and Neoproterozoic heating in the Usagaran Orogen, Tanzania, revealed by single grain 40Ar/39Ar thermochronology. Journal of African Earth Sciences 39, 165–176.

Roe, R.-J., 1965. Description of crystallite orientation in polycrystalline materials. III. General solution to the pole figure inversion. Journal of Applied Physics 36, 2024–2031.

Schmid, S.M., Casey, M., 1986. Complete fabric analysis of some commonly observed quartz *c*-axis patterns. Geophysical Monographies 36, 263–286.

Shackleton, R.M., 1973. Correlation of structures across Precambrian orogenic belts in Africa. In: Tarling, D.H., Runcorn, S.K. (Eds.), Implications of Continental Drift to the Earth Sciences. Academic Press, London, pp. 1091–1095.

Shackleton, R.M., Ries, A.C., 1984. The relation between regionally consistent stretching lineations and plate motions. Journal of Structural Geology 6, 111–117.

Sommer, H., Kröner, A., Hauzenberger, C.A., Muhongo, S., Wingate, M.T.D., 2003. Metamorphic petrology and zircon geochronology of high-grade rocks from the central Mozambique Belt of Tanzania: crustal recycling of Archean and Palaeoproterozoic materials during the Pan-African Orogeny. Journal of Metamorphic Geology 21, 915–934.

Sommer, H., Kröner, A., Hauzenberger, C., Muhongo, S., 2005a. Reworking of Archaean and Palaeoproterozoic crust in the Mozambique Belt of central Tanzania as documented by SHRIMP zircon geochronology. Journal of African Earth Sciences 43, 447–463.

Sommer, H., Kröner, A., Muhongo, S., Hauzenberger, C., 2005b. SHRIMP zircon ages for post-Usagaran granitoid and rhyolitic rocks from the Palaeoproterozoic terrain of southwestern Tanzania. South African Journal of Geology 108, 247–256.

Stern, R.J., 1994. Arc assembly and continental collision in the Neoproterozoic East African Orogen: implications for the consolidation of Gondwanaland. Annual Review of Earth and Planetary Sciences 22, 319–351.

Stipp, M., Stünitz, H., Heilbronner, R., Schmid, S.M., 2002. The eastern Tonale fault zone: a "natural laboratory" for crystal plastic deformation of quartz over a temperature range from 250 to 700 °C. Journal of Structural Geology 24, 1861–1884.

Talbot, C.J., 1999. Ductile shear zones as counterflow boundaries in pseudoplastic fluids. Journal of Structural Geology 21, 1535–1551.

Tenczer, V., Hauzenberger, C.A., Fritz, H., Whitehouse, M.J., Mogessie, A., Wallbrecher, E., Muhongo, S., Hoinkes, G., 2006. Anorthosites in the Eastern Granulites of Tanzania-new SIMS zircon U-Pb age data, petrography and geochemistry. Precambrian Research 148, 85–114.

Vail, R.J., 1985. Pan-African (Late Precambrian) tectonic terranes and reconstruction of the Arabian–Nubian Shield. Geology 13, 839–842.

Vissers, R.L.M., 1989. Asymmetric quartz *c*-axis fabric and flow vorticity: a study using rotated garnets. Journal of Structural Geology 11, 231–244.

Vogt, M., Kröner, A., Poller, U., Sommer, H., Muhongo, M., Wingate, M.T.D., 2006. Archaean and Palaeoproterozoic gneisses reworked during a Neoproterozoic (Pan-African) high-grade event in the Mozambique Belt of East Africa: structural relationships and zircon ages from the Kidatu area, central Tanzania. Journal of African Earth Sciences 45, 139–155.

Wallis, S.R., 1992. Vorticity analysis in a metachert from the Sanbagawa Belt, SW Japan. Journal of Structural Geology 14, 271–280.

Wendt, I., Besang, C., Harre, W., Kreuzer, H., Lend, H., Müller, P., 1972. Age determinations of granitic intrusions and metamorhpic events in the early Precambrian of Tanzania, In: Proceedings of the 24th International Geological Congress Montreal, vol. I, pp. 295–314.

Wenk, H.R., 1985. Measurements of pole figures. In: Wenk, H.R. (Ed.), Preferred Orientation in Deformed Metals and Rocks: An Introduction to Modern Texture Analysis. Academic Press, Orlando, pp. 11–47.